

# Optimization of FinFET-Based Gain Cells for Low Power Sub- $V_T$ Embedded DRAMs

E. Amat<sup>1</sup>, A. Calomarde<sup>1</sup>, R. Canal<sup>2</sup>, and A. Rubio<sup>1,\*</sup>

<sup>1</sup>Electronic Engineering Department, Universitat Politècnica de Catalunya (UPC), Barcelona, 08034, Spain

<sup>2</sup>Computer Architecture Department, Universitat Politècnica de Catalunya (UPC), Barcelona, 08034, Spain

(Received: 15 December 2017; Accepted: 12 February 2018)

Sub-threshold circuits (sub- $V_T$ ) are a promising alternative in the implementation of low power electronics. The implementation of gain-cell embedded DRAMs (eDRAMs) based on FinFET devices requires a careful design to achieve the maximum cell performance (i.e., retention time, access time, and energy consumption) suitable for the sub- $V_T$  operating level. In this work, we show that asymmetrically resizing the memory cell (i.e., the channel length of the write access transistor and the width of the rest of the devices) results in a 3.5× increase in retention time when compared to the nominal case while reducing area, as well. In terms of reliability (e.g., variability and soft errors), the resizing also improves the cell robustness (50% and 1.9×, respectively) when the cells are operated at sub- $V_T$  level.

**Keywords:** FinFET, eDRAM, Sub- $V_T$ , Single Event Upsets, Variability, Reliability.

## 1. INTRODUCTION

The booming of the Internet of Things (IoT) and health care applications domains<sup>1–3</sup> has increased the interest for ultra-low power circuits. In this sense, circuits that operate below the threshold voltage (sub- $V_T$  circuits) have emerged as a plausible choice. In sub- $V_T$  circuits, supply voltage ( $V_{DD}$ ) is reduced below the device threshold voltage ( $V_T$ ) to reduce the power consumption. Wireless sensor networks, medical applications and mobile signal processing<sup>2,3</sup> with medium-speed applications (kHz–MHz regime) are the most appropriate applications for such sub- $V_T$  circuits. To enhance (enlarge the drive current) of sub- $V_T$  circuits, sizing appropriately the cell devices is one of the most effective solutions.<sup>4</sup> In such systems, energy efficiency is of primary concern. The lowest energy consumption is usually achieved at the sub-threshold level, where the minimum energy point (MEP) is observed.<sup>4,5</sup> At sub- $V_T$  level, the main driving current is the sub-threshold current ( $I_{SUB}$ ), which is highly sensitive to changes in temperature and bias conditions. Performance is greatly affected by device variability, due to the devices' exponential sensitivity to source voltage,<sup>4</sup> and single event upsets (SEUs), due to its lower electric fields.<sup>6</sup>

Nowadays, beyond 32 nm technology nodes, vertical multi-gate devices (FinFETs) have replaced bulk planar devices in very large-scale integrated (VLSI) circuits in

the quest of higher density, lower power and higher performance. These devices offer several advantages that give them a high potential to push back the integration limits: lower impact on short-channel effects, steeper sub-threshold slope, lower leakage current and relevant variability reduction.<sup>7</sup> FinFETs also introduce several reliability concerns, such as the self-heating effect. On top of that, scaling down device dimensions leads to lower node capacitances and, thus, increased sensitivity to ion impacts (i.e., SEUs<sup>8</sup>). SEUs are now one of the main reliability threats for sub- $V_T$  circuits and specially for memories.<sup>6</sup> SEUs occur when an ionizing particle strikes a sensitive node (e.g., storing node), transferring energy that generates enough charge disturbances to flip a circuit node's data. To determine the robustness against SEUs, we compute the minimum charge required to upset a circuit node (i.e., the critical charge- $Q_{crit}$ ).<sup>8</sup> Initially, FinFETs provide a higher SEU robustness due to their 3D topology.<sup>9</sup> However, this advantage reduces as dimensions scale down. Plus, the use of lower  $V_{DD}$  generates small electric fields and drive currents within the cell devices, which increases vulnerability to SEUs. All of these reliability issues damage memory cell behavior. It is especially severe in SRAM as shown in Refs. [10–12]. In this context, gain-cell eDRAMs are more attractive than other memory cell proposals due to: (1) their higher density and better reliability;<sup>13,14</sup> (2) compatibility with mainstream CMOS processes; and (3) non-destructive read operations (in contrast to conventional 1T1C DRAM<sup>15</sup>). In order to

\*Author to whom correspondence should be addressed.  
Email: antonio.rubio@upc.edu

hold the data, periodic refreshes are required<sup>12</sup> as the leakage current significantly reduces the DRAM's retention time (RT).<sup>14</sup> To introduce the gain-cells in the sub- $V_T$  operating range is of great interest in areas such as biomedical applications where the power consumption of the CPU and memory accounts for 55% of the system's power.<sup>1</sup> Memory systems are usually based on SRAM cells; few studies have evaluated the use of gain-cell eDRAM-based systems at sub- $V_T$  range.<sup>3</sup> Current state of the art in sub- $V_T$  gain-cell eDRAM design mostly focuses on bulk CMOS devices. Although the continuous device dimension reduction has been questioned<sup>16</sup> and it is not trivial, FinFETs may be able to continue device scaling in smaller technologies; as shown in our previous work.<sup>17</sup>

The rest of this paper is organized as follows: Section 2 explains the device models used to simulate the FinFET gain-cell eDRAM and the simulation environment. Section 3 compares the performance and energy efficiency of different gain-cell eDRAM configurations. Section 4 reports the reliability study (variability and SEU) carried out on all the memory cells and different device types. Finally, Section 5 presents the conclusions of this work.

## 2. SIMULATION FRAMEWORK

This section presents the memory cells, the figures of merit, and the configuration parameters of the analysis.

### 2.1. Gain-Cell eDRAM Re-Design

Different eDRAM cells are usually considered to replace conventional DRAM capacitance-based cells (1T1C). 2T cells are the most likely to be implemented due to their higher integration level. Yet, 3T1D offer better reliability robustness.<sup>13</sup> In fact, 2T cells show good operability in the sub- $V_T$  range for biomedical applications.<sup>3</sup> In this context, we have focused to analyze the feasibility of FinFET-based 2T and 3T1D eDRAM cells to operate at sub- $V_T$  level. Figure 1 illustrates the schematics of the two gain-cell eDRAMs (2T and 3T1D). The baseline device to implement the gain-cell eDRAMs has always been 10 nm FinFET. These devices are based on the High-Performance Predictive Technology Models Multi-Gate (HP PTM-MG) environment.<sup>18</sup> Note that this paper

complements a previous study<sup>13</sup> for nominal  $V_{DD}$  range (0.4–1 V). This version focuses on the analysis of sub- $V_T$ -level performance;  $V_{DD}$  range is set between 0.16 and 0.3 V. When considering the complete system data path (e.g., sense amplifier, multiplexer, and flip-flop), memory cells become the critical component when variability occurs.<sup>19</sup> This is caused by their design with minimum device dimensions, which make them more susceptible to variations. Hence, we concentrate on the cell analysis. The following cell parameters are measured:

(a) *Retention Time* (RT), defined as the time required for the storage node voltage ( $V_S$ ) in the cell to decay to  $V_{Smin}$ , (the minimum cell voltage that can be read at a given frequency<sup>10</sup>). This is used as the reference parameter to analyze the cells' suitability.

(b) *Dynamic Power consumption* (PW) obtained by the average value in one read/write cycle.

(c) *Write Access Time* (WAT), defined as the time elapsed between  $V(WL_{write}) = (0.5 * V_{DD})$  and  $V_S = (0.9 * V_{DD})$ .

(d) *Read Access Time* (RAT), defined as the time elapsed between  $V(WL_{read}) = (0.5 * V_{DD})$  and  $V(BL_{read}) = (0.9 * V_{DD})$ .

Previous papers [13], [20] report a significant performance improvement in gain-cell eDRAMs when  $p$ - and  $n$ FinFET devices are properly mixed in a cell. In fact, the use of pFinFET devices for write access transistors provides a longer retention time and better robustness against variability, due to their lower leakage currents.<sup>13</sup> Note that sub- $V_T$  circuits underperform their above-threshold counterparts as the drive current ( $I_{SUB}$ ) is significantly lower. To solve this problem, devices are often resized to improve their electrical behavior.<sup>4</sup> The increment in drive strength is usually achieved by increasing the device width ( $W$ ), but it can also be achieved by increasing the channel length ( $L$ ) in the sub- $V_T$  regime.<sup>4</sup> Consequently, this paper explores the potential of upsizing the cell dimensions (i.e.,  $L$  and  $W$ ) to enhance cell performance. To this end, the following gain-cell eDRAM topologies are analyzed: (1) 2W cell, double width ( $W$ ) of the cell devices; (2) 2L, double channel length ( $L$ ) of all cell devices; (3) 2WL, double  $L$  and  $W$  of all cell devices; and, (4)  $m$ WL, double  $L$  of the write access transistor and double  $W$  of the rest of the cell devices. To double the device width in FinFET devices, we

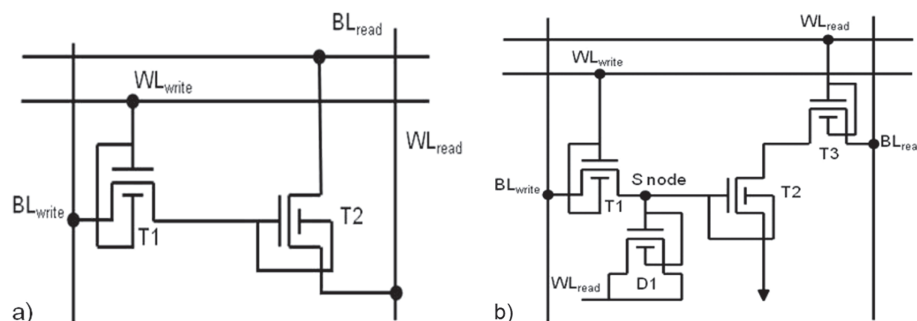


Fig. 1. Schematic structures for the gain-cell eDRAM: (a) 2T and (b) 3T1D. WL is wordline and BL is bitline.

double the number of fins in the transistor. Increasing the FinFET width means using a larger number of fins, which, in turn, leads to larger area overhead than when only the length is increased. In other words, increasing the write access device's channel length instead of its width causes a smaller increase in cell area. This smaller area overhead contrasts with the usual strategy, where the width of all devices is doubled ( $2W$ ) for sub- $V_T$  memory cells in order to improve overall performance.

**2.2. Reliability Concerns for Studying eDRAM Cell Suitability at Sub- $V_T$  Level**

The continuous reduction of technology nodes towards a nanometer regime (<32 nm) has increased the impact of reliability effects on memory-cell behavior. Moreover, in the case of circuits operating at sub- $V_T$  level, some reliability issues have taken on even more importance in terms of performance, such as process variations, changes in temperature, and soft errors.<sup>21</sup> This subsection describes the different reliability scenarios considered in the analysis of the gain-cell eDRAM's behavior.

The device fluctuation on the eDRAM cell parameters is determined by analyzing 10,000 sample Monte Carlo simulations. Experimental variability data is still not available so the variability impact is modeled by assuming a change in the threshold voltage ( $V_T$ ) of the devices in the memory cell. In this regard, the process variation level is set as a 10%  $V_T$  shift. The relevance of the variability is evaluated using a statistical distribution with mean ( $\mu$ ) and standard deviation ( $\sigma$ ), obtaining the ratio factor  $3\sigma/\mu$ , expressed as a percentage. The influence of the ambient temperature on the eDRAM performance is analyzed at -30, 25, 75 and 100 °C. Finally, all simulations take into account the self-heating effect of FinFETs through the consequent modification of the 10 nm FinFET model parameter.

To emulate SEU sensitivity of the memory cell at sub- $V_T$  level, the impact of an ion strike is simulated with a pulse wave current obtained on 10 nm FinFET technology from 3D-TCAD simulations. Figure 2(a) depicts the

**Table I.** 3D-TCAD 10 nm FinFET dimensions.

Parameter	Description	Value (nm)
$H_{Fin}$	Fin height	21
$W_{Fin}$	Fin width	9
$L_{Channel}$	Channel length	14

FinFET 3D-TCAD device designed for this study, and Table I shows its main dimensions. Unlike the nominal voltage operational range, the current induced by the radiation impact has two main components (drift and diffusion), but when circuits operate at sub- $V_T$  level, the single event effect (SEE) is mainly caused by diffusion.<sup>6</sup> In this sense, the SEU study is adapted to this concrete environment. Figure 2(b) shows the drain current pulse produced by the radiation impact of a Linear Energy Transfer (LET) of 4 MeV/mg/cm<sup>2</sup>. All SEU studies are conducted at room temperature, since temperature has a negligible effect on  $Q_{crit}$ .<sup>8</sup> Only strikes occurring in the middle of the drain region with normal incidence are considered, as these account for most of the soft error upsets, even in scaled devices. The ion characteristic radius is about 10 nm, and maximum range is 160 nm. In the context of DRAMs, the most sensitive region is the drain region of the write access transistor as it is directly connected to the storage node voltage ( $V_S$ ),<sup>13</sup> while the others are connected to the cell's word-line (WL) and bit-line (BL) (Fig. 1), which entails a high load capacitance at those nodes and, therefore, greater robustness to SEUs.

**3. eDRAM CELL PERFORMANCE AT SUB- $V_T$  RANGE**

In this section, we compare the behavior of the two types of gain-cell eDRAMs (2T and 3T1D) at sub- $V_T$  level, focusing mainly on RT. Both types of eDRAM mix  $p/n$ FinFET devices in the same cell. We also added an  $n$ FinFET-only 3T1D cell for comparison. Figure 3(a) shows the RT as a function of the  $V_{DD}$  at sub- $V_T$  level (0.16–0.3 V) for all the cells. Note that the 3T1D-eDRAM cell is implemented by two different configurations, mixed and  $n$ FinFET-only. Although the mixed-based 3T1D and 2T had a similar evolution in terms of RT with  $V_{DD}$ , the gated-diode gain cell (3T1D) yielded higher RT values (65%), as shown in Figure 3(b). These findings are consistent with previous studies<sup>13</sup> at above-threshold voltage, where the 3T1D DRAM cell had the best performance. When the nMOS-only 3T1D eDRAM cells are compared to the mixed ones, the latter significantly achieve higher RT values (20×). Consequently, the mixed 3T1D cell is used in the rest of the paper as the baseline memory cell. It is worth mentioning that the RT values obtained can still be larger when considering layout strategies such as metal stacking.<sup>3</sup> Metal stacking increases the storage node capacitance, and consequently increase the overall retention time value of the gain-cells.

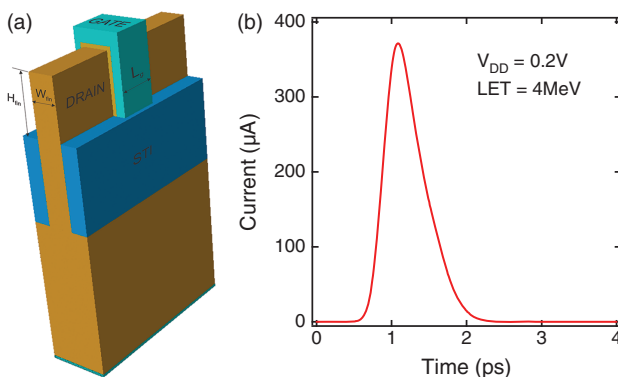


**Fig. 2.** (a) 3D-TCAD device representation. (b) Drain current pulse simulating the radiation impact on a 10 nm FinFET device.

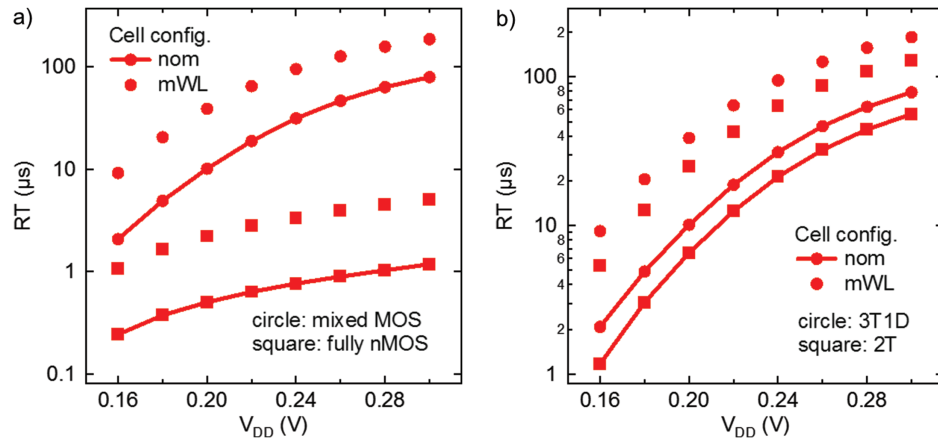


**Fig. 3.** RT of the different eDRAM cell configurations when  $V_{DD}$  is swept from 0.16 to 0.3 V under different cell scenarios: (a) Memory cell is fully implemented by nFET devices or when  $p$  and  $n$ FETs are mixed; and (b) 2T (squares) and 3T1D (circles). Mixed 3T1D cell yields higher RT values (65%) at sub- $V_T$  level than the other two proposals.

**3.1. Relevance of eDRAM Resizing Ant Sub- $V_T$  Level**

Next, we analyze the impact on RT of resizing the memory cell devices. Figure 4(a) shows that RT is higher when the cell is upsized for all of the cell proposals considered (2W, 2L, 2WL, and mWL). When only the  $W$  or  $L$  is increased, we observe a different RT trend. While the 2L cell has a better RT ( $2\times$ ) at the ultra-low  $V_{DD}$  level (0.16–0.24 V),

beyond that point, the RT values are similar to those of the nominal cell. In contrast, the opposite behavior is observed for the 2W cell: although the RT is initially almost the same as the nominal proposal, it improves ( $2\times$ ) as  $V_{DD}$  increased. It is worth noting that the RT cross-point is observed around 0.25 V, close to the threshold voltage of the 10 nm PTM pFinFET devices used in this study for

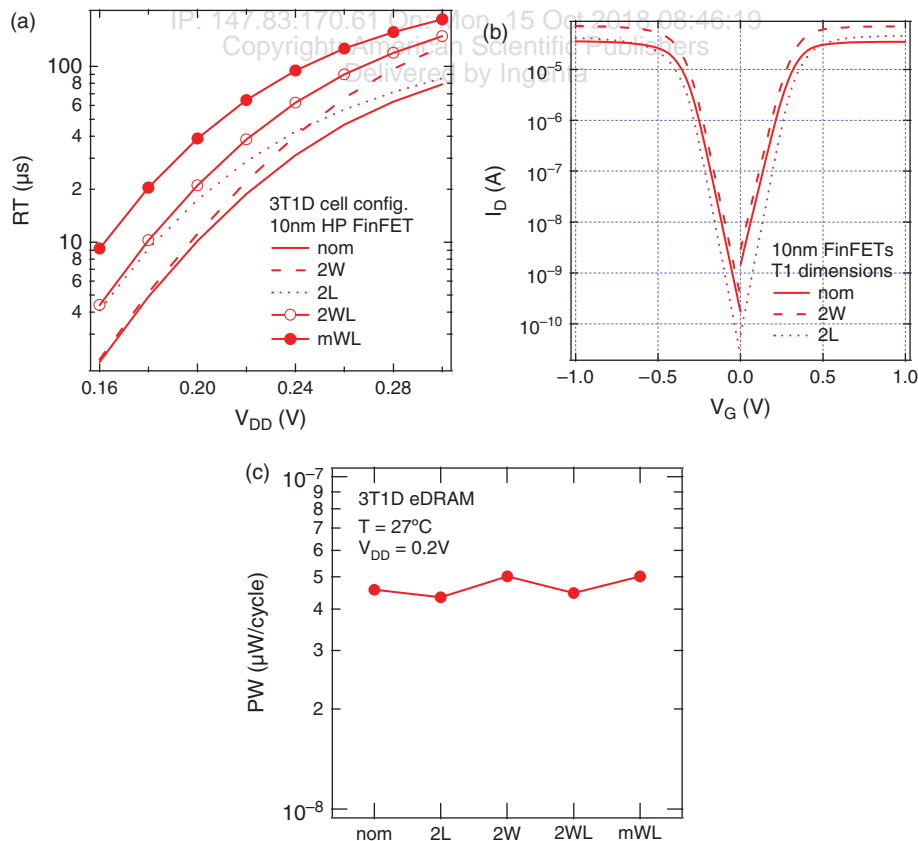


**Fig. 4.** (a) RT as a function of  $V_{DD}$  (0.16–0.3 V) when different device dimensions are considered; (b)  $I_D - V_G$  curves for 10 nm PTM  $p/n$ FinFETs for different device dimensions. (c) Power consumption of the different 3T1D-eDRAM cells resizing strategies (nominal, 2L, 2W, 2WL and mWL).

the write access transistor (Fig. 4(b)). For the  $2W$  cell, the RT shows a more uniform increase ( $2\times$ ) as compared to the nominal cell for the entire  $V_{DD}$  range. Finally, the  $mWL$  proposal shows the largest increase in RT ( $3.5\times$ ). This improved performance of the asymmetrically upsized 3T1D-eDRAM cell can be explained by the larger sub-threshold slope values and lower leakage current ( $I_{off}$ ) values (Fig. 4(b)) as  $L$  increased in the write access pFinFET. These results corroborate the largest RT values obtained when the gain-cell devices are up-scaled<sup>22</sup> in other memory cells and using different technologies. In terms of memory cell power consumption, Figure 4(c) points out no relevant difference between the 3T1D-DRAM cells with different device dimensions strategies (nominal,  $2L$ ,  $2W$ ,  $2WL$  and  $mWL$ ) when  $V_{DD}$  is 0.2 V and it operates at room temperature. So, for next studies we will mainly focus on RT evolution as it is the most relevant parameter for the suitability of the eDRAM cells at sub- $V_T$  level.

The working frequency of a memory circuit is usually determined by the longest access time, either WAT or RAT, obtained in the memory cell simulations. Then, in terms of access time, as expected, the different device dimensions resulted in different WAT and RAT values. In this context, Figure 5(a) shows the working frequency for different 3T1D-eDRAM cell proposals (nominal,  $2W$ , and  $mWL$ ). The  $2W$  configuration achieves the highest frequency due to the larger drive current resulting from the cell devices' doubled  $W$ . In contrast, the  $mWL$  proposal has the lowest frequency value, although it is still within the usual operational range ( $>100$  MHz) of sub- $V_T$  memory circuits. Please note that these values are obtained regarding the performance of a single gain-cell memory. Note that a full memory data-path is not considered in this work.

It is important to pay attention to the ambient temperature influence on the different 3T1D-eDRAM cell device size configurations, as it is usually considered a limiting factor of circuit behavior. Figure 5(b) shows how temperature variations significantly affected RT values. Ultra-low

$V_{DD}$  (sub- $V_T$ ) circuits are highly affected by the temperature increase, as the RT reduces more significantly, due to the larger relevance of the leakage current as temperatures rise, since the  $I_{SUB}$  (driving current) is highly affected by temperature. This study compared the nominal-dimension cell with the  $mWL$  proposal. In general, all the cells have longer RTs when operating at  $-30^\circ\text{C}$  (significantly so at ultra-low  $V_{DD}$ ). Likewise, all the DRAM cells shows a significant reduction in RT as the temperature rises up to  $100^\circ\text{C}$ . In particular, the  $mWL$  proposal shows less RT degradation ( $49\times$ ) as a result of ambient temperature than the nominal case ( $64\times$ ). Similar trends are observed for the 2T-eDRAM cells, but they are not plotted here to avoid redundant information.

### 3.2. Energy Efficiency of the Different Cell Proposals

A system's energy efficiency can be monitored at the circuit's minimum energy point, defined as the voltage at which the total energy consumed per operation is minimized. The MEP is equal to the minimum value of the total energy consumed by a circuit,<sup>4</sup> which is the sum of the dynamic and static energies. Dynamic energy is related to circuit-switching activity and is usually determined as  $1.2 * C * V_{DD}^2$ , where  $C$  is the switched capacitance. Static energy usually corresponds to the circuit's leakage contribution, although it is also closely related to the circuit's delay ( $V_{DD} * I_{leak} * t_d$ ).<sup>4</sup>

Figure 6 shows the different energy curves per operation depending on the  $V_{DD}$  for the baseline memory cell (3T1D) for each of the different gain-cell eDRAM proposals (i.e., nominal,  $2W$ ,  $2L$ , and  $mWL$ ). In terms of voltage at the MEP, while there are slight differences between the various cell configurations, the minimum value for all of them is around 0.2–0.22 V. Consequently, 0.2 V is used as the study's reference operating voltage for sub- $V_T$  level gain-cell eDRAM operation to ensure maximum energy efficiency. In terms of energy consumption, the value for the  $mWL$  proposal is  $\sim 30\%$  smaller than that for the  $2W$  proposal.

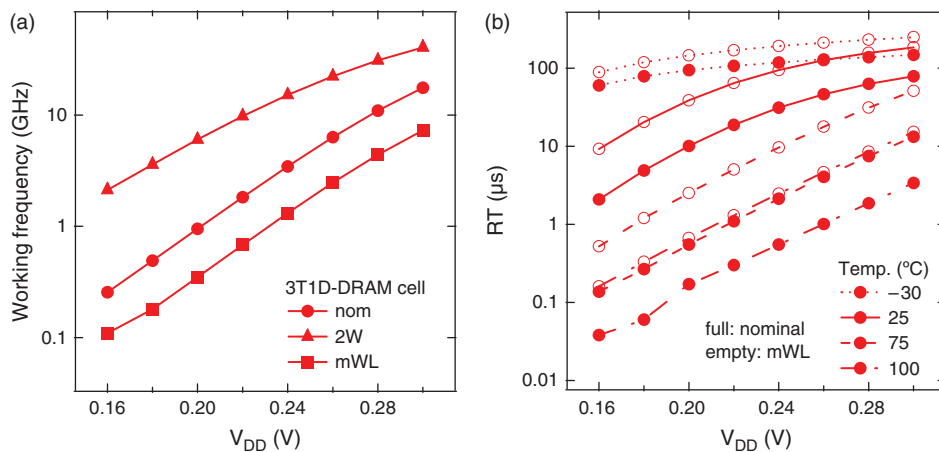
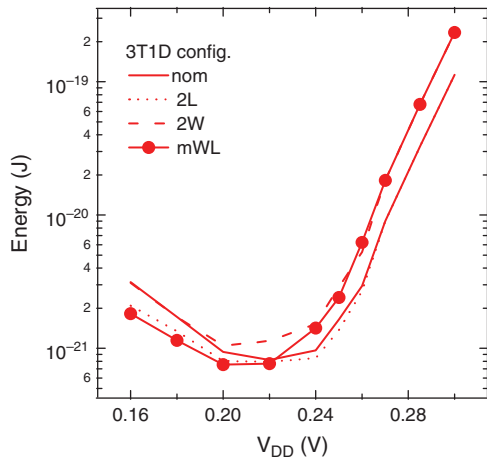


Fig. 5. (a) Working frequency considered for the different 3T1D-eDRAM cell proposals at sub- $V_T$  level; (b) influence of ambient temperature on the different cell configurations.



**Fig. 6.** Energy efficiency of the different 3T1D-eDRAM proposals (nominal, 2W, 2L, and *mWL*). Similar MEP voltages are observed for the different proposals, but energy consumption is ~30% lower for the *mWL* proposal than for the 2W one.

#### 4. RELIABILITY OF THE eDRAM CELLS AT SUB- $V_T$ LEVEL

Environmental conditions significantly affect memory cells performance and reliability, when they are designed to operate at sub- $V_T$  level. For this, we have analyzed two different reliability issues—variability and SEU—to determine the suitability of the gain-cell eDRAM to operate at sub- $V_T$  level.

##### 4.1. Influence of Variability on the eDRAM Cells at Sub- $V_T$ Level

Process variations have emerged as a relevant reliability factor as devices have been scaled into the nanometer regime. Sub- $V_T$  circuits designed at these nodes are more prone to suffer variability, making it the main reliability concern.<sup>4</sup> This section examines the impact of process variations on eDRAM cells (2T and 3T1D) performance, in particular on RT. Specifically, it looks at the impact of a moderate level of variability (10%) on 10 nm FinFET-based gain-cell eDRAM. Although memory cell speed also suffers from variability impact, we focus on RT because we have regarded as the main eDRAM cells parameter. Figure 7 shows the RT change for all the 3T1D-eDRAM cells subject to device process variation ( $3\sigma/\mu$ ) at sub- $V_T$  level ( $V_{DD} = 0.2$  V). As expected, the larger the device dimensions, the smaller the cell variability. However, RT decreases for all the resized eDRAM cells. The 2WL and *nWEL* show the smallest RT variation (~50%). Moreover, the *mWL* reduces the impact to 30% compared to the 2W with just a slightly smaller cell area. This can be attributed to the use of a longer channel length, which improves the sub-threshold slope.<sup>5</sup> It is worth to mention that 2T cells designed by using *mWL* cell configuration subjected to process variations, show larger RT variation (25%) compared to their 3T1D counterparts. This can be caused by the higher number of devices in the 3T1D and

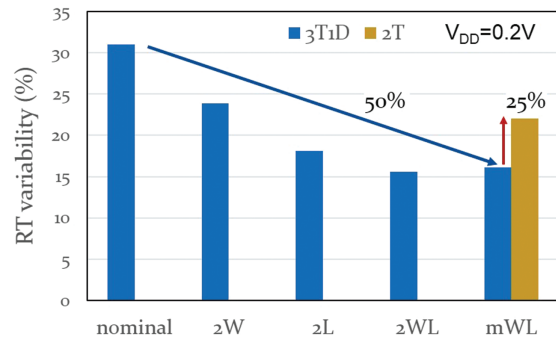


**Fig. 7.** RT deviation for the different eDRAM cell proposals subject to a 10% variability level, when operated at sub- $V_T$  level ( $V_{DD} = 0.2$  V).

the sharpened distribution obtained when gain-cell devices are up-sized.<sup>22</sup> For a more realistic analysis, we compute the manufacturing yield of a 32 kB cache memory block based on 3T1D cells, in a 10% variability scenario and operating at sub- $V_T$  level ( $V_{DD} = 0.2$  V). For this purpose, the circuit is evaluated with a reconfigurable array of 512 cells per column, for 512 columns, followed by 24 redundant columns.<sup>23</sup> In this context, 3T1D-eDRAM cells with RTs lower than 714 ns are considered defective, as such an RT value only ensures that the performance loss in a system based on 3T1Ds will be within ~2% of an ideal 6T design.<sup>12</sup> Figure 8 shows the results for the 32 kB 3T1D-eDRAM memory blocks based on the different cell upsizing proposals; all of them achieved a 99% yield under 10% device variability at room temperature (25 °C). When the ambient temperature changes, the retention time of the 32kB block falls significantly; and while at 75 °C (squares) only the *mWL* proposal meets the time criterion, at 100 °C (triangles) none of them do. This RT limit

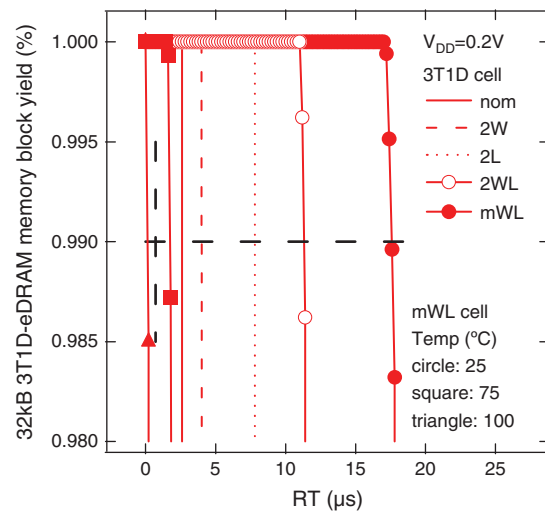


**Fig. 8.** Yield behavior for a 32 kB memory block based on 10 nm FinFET-based 3T1D cells subject to a 10% variability level for each of the different cell proposals (nominal, 2W, 2L, 2WL, and *mWL*) at sub- $V_T$  level ( $V_{DD} = 0.2$  V). Additionally, studies at high temperatures for the *mWL* 3T1D-eDRAM proposals are shown. Although the 32kB memory block met the timing criterion, 714 ns, at 75 °C (squares), at higher temperatures (100 °C, triangles) it did not.

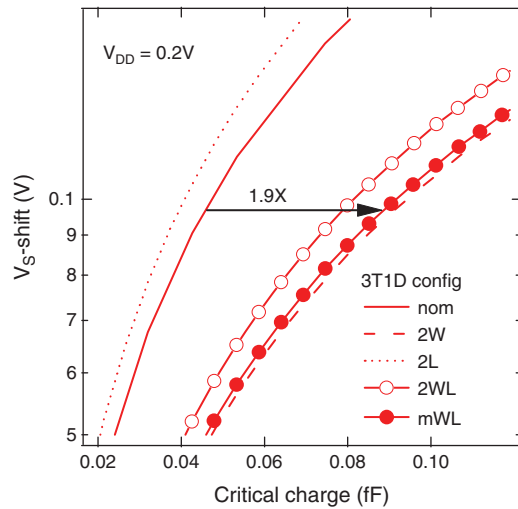


**Fig. 9.** Study of SEU impact on 3T1D-eDRAM cells. When using different device dimensions, larger injected charges are required to obtain a  $V_S$ -shift of  $V_{DD}/2$  for the  $mWL$  configuration.

(714 ns) may seem a very aggressive regarding the refresh period, but there are different proposals for “refresh-free” cells, dual-ported memories, and other refresh optimization techniques.<sup>12, 18</sup>

#### 4.2. Impact of SEUs on the eDRAM Cells

In the context of SEU analysis, only those ion impacts occurring in the drain region are considered (see Section 2.2). In particular, the devices connected to the storage node are the weakest, as they are the most sensitive node of the circuit. Thus, the only device significantly affected by an ion strike is the write access device, as the other devices are either connected to high capacitance lines, i.e., the bit-line (BL) and word-line (WL), or they exhibit a low influence on the cell performance following an ion impact.<sup>13</sup> Hence, we compare the relevance of the different configurations of upsized device dimensions used to implement the gain-cell eDRAMs at sub- $V_T$  level ( $V_{DD} = 0.2$  V). In this context, Figure 9 shows the influence of the device dimensions (nominal,  $2W$ ,  $2L$ ,  $2WL$ , and  $mWL$ ) when considering a  $V_S$ -shift of  $V_{DD}/2$  (i.e., loss of the stored data) as opposed to the critical charge required upsetting the node. In this regard, the  $mWL$  and  $2W$  proposals are the most robust, as they have a larger  $Q_{crit}$  ( $\sim 1.9\times$ ). This is related to the influence of the upsized transistors in the SER, specifically for the  $W$  increase.<sup>8</sup> Although the same trend ( $1.8\times$ ) is observed for the 2T-DRAM (not included in the figure), the critical charge required to upset the node is smaller (50%), as previously reported in Ref. [13], indicating the higher robustness of the 3T1D memory cells to SEU.

## 5. CONCLUSIONS

Gain-cell eDRAMs for sub- $V_T$  operation have been presented as a suitable option for ultra-low power

memory systems. The best gain-cell device configuration mixes  $p$ - and  $n$ FinFET devices. This configuration can achieve  $20\times$  higher RT at the sub- $V_T$  operational level when compared to other alternatives. Per-device resizing also improves the RT of the cell for the FinFET-based cells at sub- $V_T$  level. The best resizing comes with doubling the channel length of the write access transistor and the width of the rest of the devices ( $mWL$  proposal).  $mWL$  yielded the highest RT ( $3.5\times$ ), due to its better subthreshold slope and the lower leakage. This proposal ( $mWL$ ) entailed lower area overhead than the conventional strategy ( $2W$ ). In terms of power consumption no significant impact is observed for the different cell configurations. Considering the working frequency, the  $mWL$  matches the usual values of the sub- $V_T$  circuits ( $\sim 100$  MHz). The  $mWL$ -based 3T1D proposal shows a larger tolerance to operating at higher temperatures. The MEP is  $\sim 0.2V$   $V_{DD}$  for all the 3T1D cell proposals, but the  $mWL$  configuration consumes 30% less energy. In terms of process variations on sub- $V_T$  3T1D-eDRAM cells, the  $mWL$  proposal shows greater robustness (50%). In a 32 kB memory block configuration, the minimum RT criterion (714 ns) is met even at high ambient temperatures (75 °C). Finally, in relation to SEUs, the  $mWL$  proposal shows to be  $1.9\times$  more robust, due to the larger critical charge required to upset the information node.

Summarizing, the asymmetrically sized gain-cell eDRAM implemented with 10 nm FinFET devices offers a clear improvement in terms of cell performance and reliability at sub- $V_T$  level and for low power consumption memory cells.

**Acknowledgments:** This work received support from the 2012 Intel Early Career Faculty Honor program and was partially funded by the Spanish Ministry of Economics and Competitive (MINECO) and the European Regional Development Fund (ERDF) (TEC2013-45638-C3-2-R).

## References

1. A. Y. Dogan, J. Constantin, M. Ruggiero, A. Burg, and D. Atienza, Multi-core architecture design for ultra-low-power wearable health monitoring systems, *DATE Conference and Exhibition* (2012), pp. 988–993.
2. D. Bol, J. de Vos, C. Hocquet, F. Botman, F. Durvaux, S. Boyd, D. Frandre, and J.-D. Legat, SleepWalker: A 25-MHz 0.4-V Sub-mm<sup>2</sup> 7- $\mu$ W/MHz microcontroller in 65-nm LP/GP CMOS for low-carbon wireless sensor nodes, *IEEE J. Solid-State Circuits* 48, 20 (2012).
3. P. Meinerzhagen, A. Teman, R. Gitterman, A. Burg, and A. Fish, Exploration of sub- $V_T$  and near- $V_T$  2T gain-cell memories for ultra-low power applications under technology scaling. *J. Low Power Electron. Appl.* 3, 54 (2013).
4. S. Hanson, B. Zhai, M. Seok, B. Cline, K. Zhou, M. Singhal, M. Minuth, J. Olson, L. Nazhandali, T. Austin, D. Sylvester, and D. Blaauw, Exploring variability and performance in a sub-200-mV processor. *IEEE J. Solid-State Circuits* 43, 881 (2008).
5. D. Bol, R. Ambroise, D. Flandre, and J.-D. Legat, Interests and limitations of technology scaling for subthreshold logic. *IEEE Trans. VLSI Syst.* 17, 1508 (2009).

6. M. C. Casey, B. L. Bhuvu, S. A. Nation, O. A. Amusan, T. D. Loveless, L. W. Massengill, D. McMorrow, and J. S. Melinger, Single-event effects on ultra-low power CMOS circuits. *IEEE IRPS* 194 (2009).
7. T. Matsukawa, Y. Liu, S.-I. O'uchi, K. Endo, J. Tsukada, H. Yamauchi, Y. Ishikawa, H. Ota, S. Migita, Y. Morita, W. Mizubayashi, K. Sakamoto, and M. Masahara, Comprehensive analysis of Ion variation in metal gate FinFETs for 20 nm and beyond. *IEEE IEDM* (2011), pp. 23.5.1–23.5.4.
8. T. Heijmen, D. Giot, and P. Roche, Factors that impact the critical charge of memory elements. *IEEE Int. On-Line Test. Symp.* (2006), pp. 57–62.
9. V. Cristofori, F. Da Ros, Y. Ding, A. Shen, A. Gallet, D. Make, G.-H. Duan, L. K. Oxenloewe, and C. Peucheret, Soft error susceptibilities of 22 nm tri-gate devices. *IEEE Trans. Nucl. Sci.* 59, 2666 (2012).
10. W. Luk, J. Cai, R. Dennard, M. Immediato, and S. Kosonocky, A 3-transistor DRAM cell with gated diode for enhanced speed and retention time. *Symp. VLSI Circuits* (2006), pp. 184–185, 10.1109/VLSIC.2006.1705371.
11. E. Amat, E. Amatl l, S. G mez, N. Aymerich, C. G. Almud ver, F. Moll, and A. Rubio, Systematic and random variability analysis of two different 6T-SRAM layout topologies. *Microelectronics J.* 44, 787 (2013).
12. X. Liang, R. Canal, G.-Y. Wei, and D. Brooks, Replacing 6T SRAMs with 3T1D DRAMs in the L1 data cache to combat process variability. *IEEE Micro* 28, 60 (2008).
13. E. Amat, A. Calomarde, F. Moll, R. Canal, and A. Rubio, Feasibility of the embedded DRAM cells implementation with FinFET devices. *IEEE Trans. Comput.* 65, 1068 (2016).
14. K. C. Chun, P. Jain, J. H. Lee, and C. H. Kim, A sub-0.9 V logic-compatible embedded DRAM with boosted 3T gain cell, regulated bit-line write scheme and PVT-tracking read reference bias. *Symp. VLSI Circuits* (2009), pp. 134–135.
15. M.-T. Chang, P. Rosenfeld, S.-L. Lu, and B. Jacob, Technology comparison for large last-level caches (L3Cs): Low-leakage SRAM, low write-energy STT-RAM, and refresh-optimized eDRAM. *IEEE International Symposium on High Performance Computer Architecture (HPCA)* (2013), pp. 143–154, 10.1109/HPCA.2013.6522314.
16. S. Ganapathy, A. Teman, R. Giterman, A. Burg, and G. Karakonstantis, Approximate computing with unreliable dynamic memories. *IEEE Int. New Circuits Syst. Conf.* (2015), pp. 1–4.
17. E. Amat, A. Calomarde, R. Canal, and A. Rubio, Suitability of FinFET introduction into eDRAM cell for operate at sub-threshold level. *Int. Symp. Power Timing Model. PATMOS* (2017), pp. 1–6.
18. S. Sinha, G. Yeric, V. Chandra, B. Cline, and Y. Cao, Exploring sub-20 nm FinFET designs with predictive technology models. *DAC Proc.* 283, 4624 (2012).
19. E. Amat, A. Calomarde, R. Canal, and A. Rubio, Variability impact on on-chip memory data paths. *European Workshop VARI* (2014), pp. 1–5.
20. K. C. Chun, P. Jain, T.-H. Kim, and C. H. Kim, A 667 MHz logic-compatible embedded DRAM featuring an asymmetric 2T gain cell for high speed on-die caches. *IEEE J. Solid-State Circuits* 47, 547 (2012).
21. M. Bagatin, S. Gerardin, A. Paccagnella, C. Andreani, G. Gorini, and C. D. Frost, Temperature dependence of neutron-induced soft errors in SRAMs. *Microelectron. Reliab.* 52, 289 (2012).
22. N. Edri, P. Meinerzhagen, A. Teman, A. Burg, and A. Fish, Silicon-proven, per-cell retention time distribution model for gain-cell based eDRAMs. *IEEE Trans. Circuits Syst. I Regul. Pap.* 63, 222 (2016).
23. S. Mukhopadhyay, H. Mahmoodi, and K. Roy, Modeling of failure probability and statistical design of SRAM array for yield enhancement in nanoscaled CMOS. *IEEE Trans. Comput. Des. Integr. Circuits Syst.* 24, 1859 (2005).

Copyright: American Scientific Publishers  
Delivered by Ingenta

### Esteve Amat

Esteve Amat received the B.S., M.S., and Ph.D. degrees in electronic engineering from the Universitat Aut noma de Barcelona in 2004, 2006, and 2009, respectively. Thanks to win a competitive grant (Juan de la Cierva) from the Spanish minister he joined to UPC in 2011, where his main task was analyze the reliability of memory cells. He was with CEA-Leti from 2014 to 2015 for a one-year research stay focused on the reliability of asynchronous circuits. In 2016, he joined the Barcelona Microelectronic Institute to collaborate on the Ions4SET EU project, where his main task in to design the process flow to manufacture a single-electron transistor.

### Antonio Calomarde

Antonio Calomarde received the B.S. degree in telecommunications engineering from the Universitat Polit cnica de Catalunya (UPC), Barcelona, Spain, in 1986; the M.S. degree in electronic engineering from the Universitat Aut noma de Barcelona, in 1993; and the Ph.D. degree in electronic engineering from the UPC in 2007. He is currently a Full-Time Associate Professor with the Department of Automatic Control, UPC. His research interests include low power/high performance digital circuits and soft error resilient circuits.

### Ramon Canal

Ramon Canal received his M.S. and Ph.D. degrees from the Universitat Polit cnica de Catalunya (UPC), in Barcelona, Catalonia, EU. He joined the faculty of the Computer Architecture Department of UPC in 2003. He finished his M.S. in the University of Bath (UK), worked at Sun Microsystems in 2000, and was a Fulbright visiting scholar at Harvard University in 2006/2007. His research focuses on power and thermal aware architectures, as well as reliability and memory hierarchy. He has an extensive list of publications and several invited talks. He has been program committee member in several editions of HPCA, ISCA, MICRO, HiPC, IPDPS, ICCD, ICPADS, CF. He has been co-general chair of HPCA 2016 and IOLTS 2012. He is a senior member of the IEEE.

### Antonio Rubio

Antonio Rubio received the M.S. and Ph.D. degrees from the Industrial Engineering Faculty of Barcelona. He has been Associate Professor of the Electronic Engineering Department at the Industrial Engineering Faculty (UPC) and professor of the Physics Department at the Balearic Islands University. He is currently professor of Electronic Technology at the Telecommunication Engineering Faculty in the Polytechnical University of Catalonia, UPC, Barcelona. His research interests include VLSI design and test, device and circuit modeling, high speed circuit design reliability and new emergent nanoarchitectures.